

PREDICTIONS ON THE DYNAMIC BEHAVIOUR OF A ROLLING ELEMENT AUXILIARY BEARING FOR ROTOR/AMB SYSTEMS

Matthew O T Cole, Patrick S Keogh and Clifford R Burrows
Department of Mechanical Engineering, University of Bath, Bath BA2 7AY, UK
ensmc@bath.ac.uk, enspsk@bath.ac.uk, enscrib@bath.ac.uk

ABSTRACT

Accurate prediction of auxiliary bearing dynamic behaviour is important for determining not only the rotordynamic response following rotor touchdown but also the likelihood of wear or damage to the bearing itself. This paper presents results obtained through theoretical modelling of a deep-groove ball bearing following rotor impact. The dynamic conditions during rotor touchdown can be deduced from equations of motion for the bearing components with component contact models that include realistic traction characteristics. Solutions obtained for the bearing component motion allow investigation of the influence of bearing design parameters on both the bearing acceleration and frictional energy dissipation within the bearing. The solutions obtained are found to be sensitive to the exact friction law used in the model, suggesting that optimisation of lubrication and friction surfaces is critical for achieving improvements in auxiliary bearing performance. This study enables increased understanding of the dynamic conditions that can occur during acceleration of the bearing, and provides a theoretical insight into how bearing design parameters and lubrication influence performance.

INTRODUCTION

The use of rolling element bearings for auxiliary operation is widespread in rotating machinery with magnetic bearings. Standard rolling element bearings are often chosen for auxiliary purposes as they provide a low maintenance solution that is cheap and easy to replace once damaged or worn. However, the mode of operation of such bearings is fundamentally different to that originally intended and designed for. For this reason there is, as yet, no satisfactory or reliable means to predict the, often limited, operational effectiveness

and service life of rolling element auxiliary bearings. To date little empirical information on the performance and reliability of auxiliary bearings has been published, whether from research or field based studies. However, some reported incidents of auxiliary bearing damage and failure have not been adequately explained and suggest that a number of interacting dynamic processes may be involved.

Many previous studies on rotor-auxiliary bearing touchdown have concentrated on the non-linear dynamic response of the rotor and the corresponding rotor-bearing interaction forces [1-6]. A major concern during rotor-auxiliary bearing contact is the possibility of friction induced backward whirl of the rotor, which produces very high bearing reaction forces [6]. Numerical simulation of a flexible rotor within an auxiliary clearance bearing [5] has provided indication of suitable radial clearances, support stiffness and damping that must be chosen to avoid such rotor dynamic behaviour.

OPERATION OF ROLLING ELEMENT AUXILIARY BEARINGS

Following initial contact between the rotor and auxiliary bearing inner race, sliding friction between the contacting surfaces causes the bearing to accelerate until the surface velocities at the contact are equal. At that time, the bearing stops accelerating and the frictional torque drops to normal levels. Consequently, an auxiliary bearing that can accelerate rapidly will be less likely to induce rotor backward whirl.

Bearing acceleration is directly related to the frictional energy losses that occur at sliding contacts, both between the rotor and inner race and between the bearing races and rolling elements. With all sliding contacts, the release of heat energy produces transient

thermal conditions that may lead to significant thermal distortion of the bearing components. Determining the contribution of thermal effects to auxiliary bearing failure is therefore an important objective.

To predict transient motion of bearing components under conventional usage simulation models have been used [7,8], which involve direct integration of the equations of motion. To model the extreme conditions that occur in auxiliary bearings, while avoiding computationally intensive integration routines, the authors have developed an alternate modelling technique [9]. This was applied to a deep groove ball bearing for which dynamic conditions during rotor touchdown were obtained by solving a set of matrix equations obtained from the equations of motion for the bearing rolling elements. To predict radial ball loads, this method also coupled a finite element (FE) model of a flexible inner race with non-linear ball stiffnesses that arise from ball-race contact distortions.

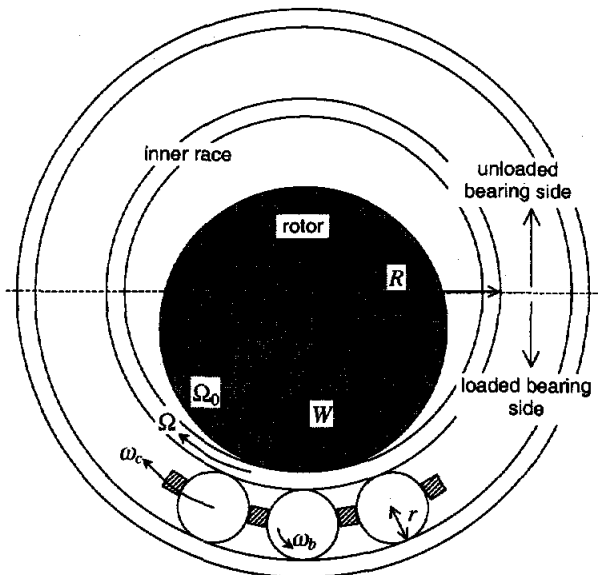


FIGURE 1: Deep groove auxiliary ball bearing with ball separator during rotor touchdown

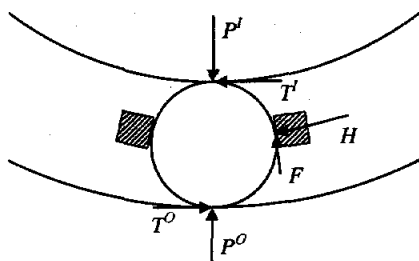


FIGURE 2: Contact forces acting on a ball

Model elements

A general model for the dynamics of an axially symmetric bearing (Fig. 1) in two dimensions can be assembled from the individual component equations of motion. For a bearing with a ball separator the equation for rotation of the j^{th} ball (mass m_b and radius r) about its centre of mass is (Fig. 2)

$$I_b \dot{\omega}_{b_j} = r(T_j^I + T_j^O - F_j) \quad (1)$$

where $I_b = \frac{2}{5} m_b r^2$. The circulatory motion of each ball is determined by the separator velocity ω_c and so the equation for circulatory motion is

$$m_b R(1+s)^2 \dot{\omega}_c = T_j^I - (1+2s)T_j^O + \cos(\alpha/2)(1+s)H_j \quad (2)$$

where R is the inner race radius and $s = r/R$ and α is the angular separation of adjacent balls. Similarly, for radial motion of each ball:

$$\frac{m_b R \Omega^2}{4(1+s)} = P_j^O - P_j^I - \cos(\alpha/2)F_j \quad (3)$$

If at least one ball is close to rolling, the angular accelerations for inner race and circulatory motion are related by $\dot{\omega}_c = \dot{\Omega}/2(1+s)$ [10]. Therefore, the equation for motion of the ball separator is

$$m_c R(1+s) \dot{\omega}_c = -\sum_j H_j \quad (4)$$

The final bearing component is the inner race, for which

$$I_i \dot{\Omega} = (R-d)\mu W - R \sum_{j=1}^N T_j^I \quad (5)$$

where μ is the coefficient for sliding friction between the rotor and bearing, I_i is the inertia of the inner race and d its thickness. Equations (1-5) can be combined into a single matrix equation including all the balls. To then solve this equation requires three further relations. Firstly the ball contact forces at the outer race P^I must be calculated for a given rotor contact force W . Results of FE modelling [9] show that, to a good approximation,

$$P_j^I = g(\theta_j)W \quad (6)$$

where θ_j is the angular position of the j^{th} ball relative to the rotor contact, and the function $g(\cdot)$ can be identified for a given bearing using FE modelling results. In addition, the pattern of ball spin speeds ω_{b_j} must be related to spin accelerations $\dot{\omega}_{b_j}$, which can be achieved using a finite difference approximation [9]:

$$\dot{\omega}_{b_j} = \dot{\Omega} \omega_{b_j} / \Omega + \omega_c (\omega_{b_j} - \omega_{b_{j-1}}) / \alpha \quad (7)$$

Finally, a suitable traction model must be included to relate normal and traction forces at every component contact. A general non-linear relation can be considered for the ball-race contacts:

$$\begin{aligned} T_j^I &= t^I(P_j^I, \omega_{b_j}, \omega_c) \\ T_j^O &= t^O(P_j^O, \omega_{b_j}, \omega_c) \end{aligned} \quad (8)$$

Similarly, for the traction due to sliding at the ball-ball or ball-separator contacts:

$$F_j = f(H_j, \omega_{b_j}, \omega_{b_{j+1}}) \quad (9)$$

Solution of equation (1-9) can be achieved using a suitable iterative method [9]. In this way, the instantaneous ball spin speeds, contact forces and overall bearing acceleration can be obtained for any instantaneous rotor contact force W and bearing speed Ω .

Qualitative findings

Initial studies using this model highlighted a number of characteristics that are unique to auxiliary bearing operation. Typically, auxiliary bearings are mounted inside the stator housing and the rotor makes direct contact with the bearing inner race. Due to the radial clearance, the flexibility of the inner race has a direct influence on the maximum ball-race contact stress that can occur. With a typical race thickness, the maximum ball-race contact stress is around twice that for the equivalent shaft mounted bearing under the same load. Increasing inner race thickness, or introducing an inner sleeve, can alleviate this problem, but will increase bearing inertia and slow bearing spin-up.

To model component contact tribology, a linear creep relation was used together with coulomb friction for gross sliding (Fig. 3a), appropriate to dry contacts. With such a traction model it was found that during bearing acceleration the spin speed of each ball oscillates as the ball orbits the bearing. This can create two distinct zones of rolling and sliding balls, on the loaded and unloaded side of the bearing respectively. Moreover, at high bearing accelerations the balls may stop spinning completely when on the lightly loaded side of the bearing. This can be attributed to the effect of friction at the contacts between adjacent balls (or between the balls and separator, if present).

MODEL BEHAVIOUR

To further investigate the behaviour of the auxiliary bearing model a number of different cases are now considered. Each case is based on a standard high-speed deep groove ball bearing (Table 1), with the following variants

Bearing A: Full complement of balls (40) without separator. Dry friction contact model (Fig. 3a).

Bearing B: Full complement of balls (40) without separator. EHL-based traction model, appropriate for lubricated contacts (Fig. 3b).

Bearing C: Ball separator included with 30 balls. Dry friction contact model.

Bearing D: Ball separator included with 30 balls. EHL-based traction model, appropriate for lubricated contacts.

Using the described models, solutions for the dynamic conditions within the bearing were obtained for an instantaneous rotor contact force of 2000N. The predicted acceleration of the bearing varies significantly with rotational speed, as shown in Fig. 4 for the cageless bearing with a full complement of 40 balls. The acceleration $\ddot{\Omega}$ is shown as a fraction of the maximum possible acceleration (with zero internal losses). For the dry bearing, the predicted acceleration falls to zero between 100 and 1000 rad/s. Over this speed range, a steady increase occurs in the number of balls that are sliding at the race contacts. At higher speeds, no steady solution could be obtained until the bearing speed exceeded 2000 rad/s, above which a different type of solution exists with all the balls rolling. The low speed and high speed solutions obtained for Bearing A are compared in Fig. 5, which shows the interaction forces between adjacent balls H and also the ball-race slip speed as a fraction of the rolling speed. All plots show the variation with ball position ($\theta = 0$ being directly under the rotor contact point). At the lower speed (100 rad/s) it is apparent that the balls stop rolling when on the unloaded side of the bearing (positions 10-30). At high speeds (3000 rad/s) all the balls are rolling, however, the ball-ball interaction forces are significantly higher and consequently the frictional losses within the bearing are also higher.

TABLE 1: Bearing parameters

Inner race radius	R	40.0 mm
Inner race thickness	d	5.0 mm
Inner race width	w	20.0 mm
Inner race inertia	I_I	$2.58 \times 10^{-4} \text{ kgm}^2$
Ball radius	r	3.4 mm
Ball mass	m_b	0.0013 kg
Number of balls	N	30/40
Rotor-race clearance	c	0.75 mm
Young's modulus	E	$2.28 \times 10^{11} \text{ N/m}^2$
Coefficient of rotor-race sliding friction	μ	0.1
Ball angular separation	α	0.209/0.157 rad

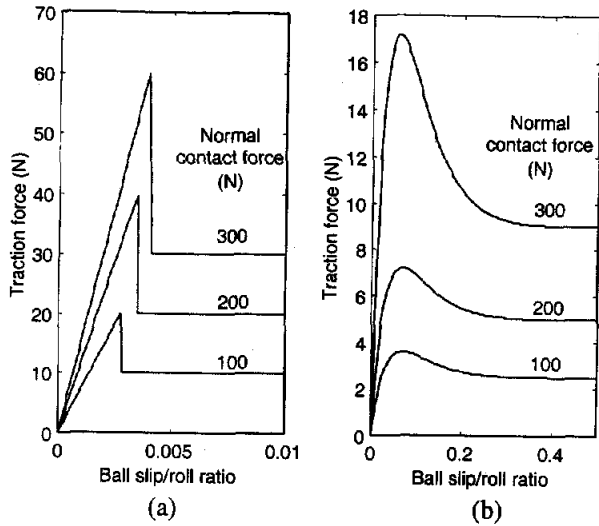


FIGURE 3: Traction characteristics for ball-race contact at bearing speed $\Omega = 1000$ rad/s (a) dry friction model (b) EHL-based model

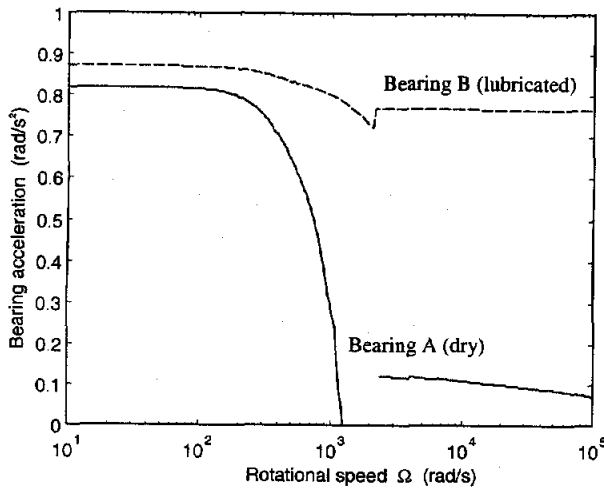


FIGURE 4: Normalised bearing acceleration as a function of instantaneous bearing velocity with rotor contact force $W = 2000$ N

The results for bearing B with the EHL contact model show a similar trend (Fig. 4), although the solution obtained for the acceleration shows a more continuous transition from the low speed to the high speed regime, and the acceleration of the bearing does not drop as significantly.

The same conditions were used to obtain solutions for bearing C and D, which both included a ball separator (Fig. 6). The variation in the bearing acceleration with speed is very small over the speed range considered. Correspondingly, the interaction forces between the balls and separator also show little variation with speed, although the variation in ball spin speeds is similar to bearing A and B.

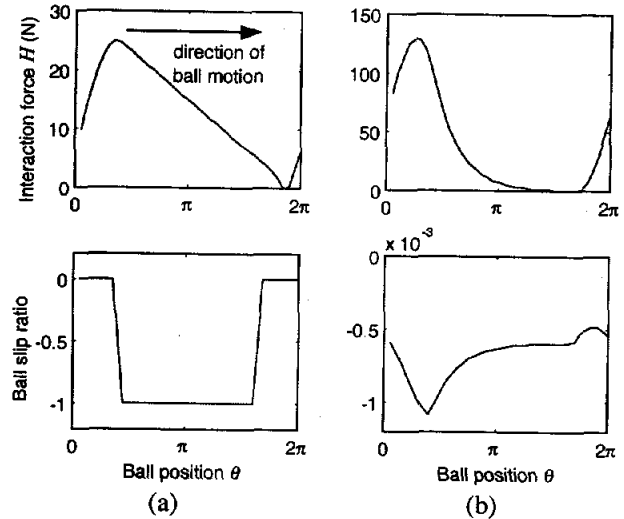


FIGURE 5: Ball interaction forces and spin speeds for bearing A as a function of ball position under rotor contact force $W = 2000$ N, at (a) $\Omega = 100$ rad/s (b) $\Omega = 3000$ rad/s

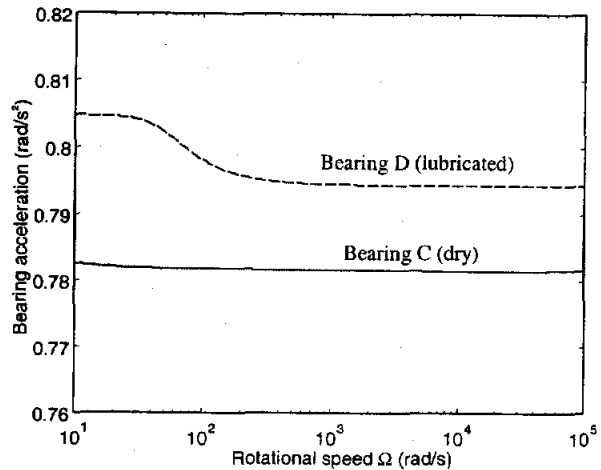


FIGURE 6: Normalised bearing acceleration as a function of instantaneous bearing velocity with rotor contact force $W = 2000$ N

For each bearing, the acceleration under a given rotor-inner race contact force is determined by the magnitude of frictional energy dissipation at the sliding contacts within the bearing. To gain a conceptual understanding of how this influences overall bearing motion, ball contact forces can be considered for a typical ball on the side of the bearing where ball loading is low (Fig. 7). At low speeds the dominant forces acting on the ball arise from separator contact and consequently the ball is 'pushed' around by the ball separator (Fig. 7a). Conversely, the balls on the loaded side of the bearing must push the separator. At higher speeds, ball centrifugal forces cause increased reaction forces P^o at the outer race (Fig 7b). The associated traction force T^o

acts to decelerate the ball orbital motion and must be overcome by a higher ball-separator force H . Consequently, at higher speeds the friction at the ball-separator contact F becomes higher and the overall acceleration of the bearing is lower.

SIMULATION RESULTS

The dependency of bearing acceleration on bearing speed has important consequences for the spin-up response of the bearing during rotor touchdown. These implications are illustrated by transient response simulations obtained for a constant rotor contact force (Fig. 8 and Fig. 9). The required bearing velocity for rolling contact with the rotor was set to 3000 rad/s (although in general this will be a function of rotor speed and motion). Even with a rotor contact force of 4000 N, it is apparent that bearing A cannot attain full speed and stops accelerating at 1800 rad/s (Fig. 8). At this speed the heat generation within the bearing will be equal to the rate of work performed by the rotor at the bearing contact. Bearing B reaches full speed with the same rotor contact forces, although the initial magnitude of acceleration is similar (Fig. 9).

IMPLICATIONS

The results of the modelling and simulation study suggest that the performance of an auxiliary bearing, in terms of the frictional losses and resultant acceleration, is highly dependent on how circumferential forces are transmitted between balls during bearing acceleration. These circumferential forces are a consequence of the orbital acceleration of the balls and must either be transmitted by a ball separator or directly between balls. In either case, gross sliding will occur at the contacts and associated frictional losses will depend on the surface-lubricant tribology.

The results obtained for the full complement bearing with the dry friction model (Bearing A) suggest that the bearing may stop accelerating completely during spin-up. The consequences for thermal conditions within the bearing or the dynamics of the rotor may be catastrophic if this were to occur in practice. Even if the bearing continued to accelerate, the frictional losses within the bearing are predicted to be many times higher in the high speed regime than at low speeds and achieving heat dissipation may be problematic.

It is clear that the introduction of a suitable oil-based lubricant (Bearing B) should alleviate this problem, however, it should be remarked that in certain applications, the surrounding gaseous conditions mean that oil-based lubricants are not an option.

The use of a ball separator or cage clearly improves the spin-up behaviour of the bearing, irrespective of the lubrication model used. However, a number of possible

disadvantages of using ball separators should be highlighted. Firstly, a bearing with a separator has fewer balls than a similarly sized full complement bearing and consequently a lower load capacity. Secondly, both the dynamics of the separator and its structural integrity under acceleration loading give cause for concern.

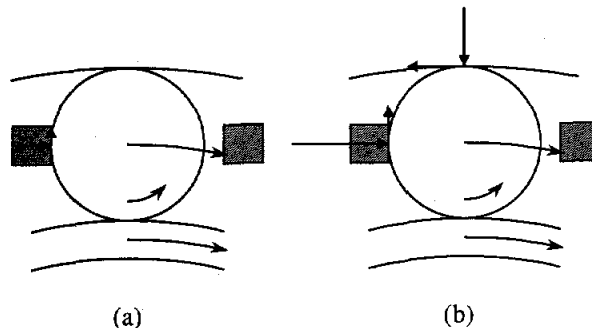


FIGURE 7: Typical ball on unloaded side of bearing. Contact force magnitudes are indicated for (a) low and (b) high bearing speed Ω .

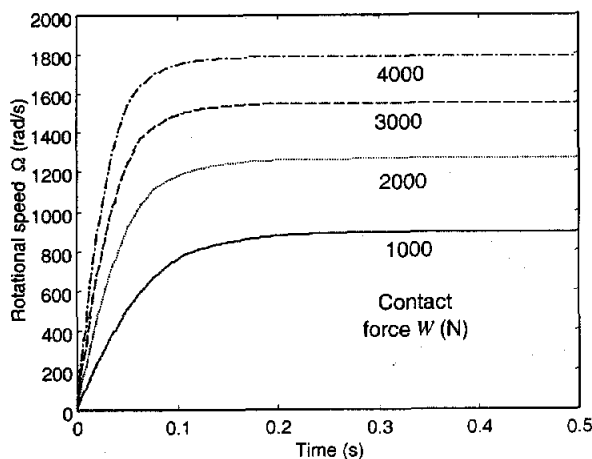


FIGURE 8: Bearing A response under constant rotor contact force W

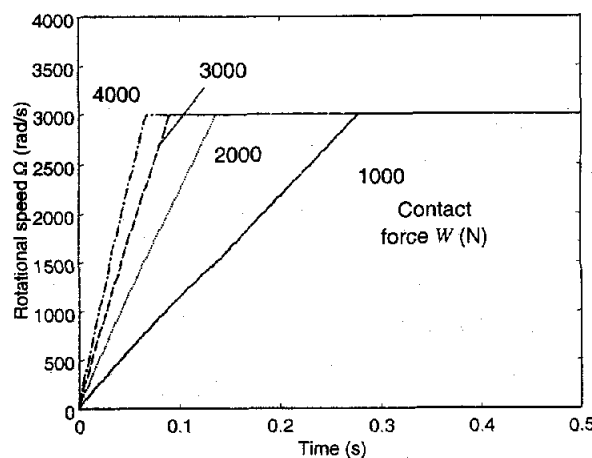


FIGURE 9: Bearing B response under constant rotor contact force W

Consider, for example, bearing C with a rotor contact force of 10000 N. The acceleration of the bearing with this force is predicted to be around $1.2 \times 10^5 \text{ rad/s}^2$. If it is assumed that all the force required to achieve orbital acceleration of the 15 balls on the unloaded side of the bearing is transmitted through the ball separator, then this force will be given by

$$15m_b \times \dot{\Omega}R/2 \approx 50 \text{ N}$$

The magnitude of this force is not negligible at high accelerations and may produce significant distortion of a lightweight separator. This may present a conflict in auxiliary bearing design, as a low inertia separator allows the bearing to accelerate faster, but consequently the separator must also have higher strength.

CONCLUSIONS

This paper has presented results from theoretical modelling of the dynamics of rolling element auxiliary bearings. The results allow a number of factors to be identified that influence the bearing spin-up behaviour. In general the acceleration of the bearing decreases with increasing speeds. This decrease in acceleration was found to correlate with the increase in magnitude of interaction forces between adjacent balls and the associated friction forces. Consequently, the inclusion of a ball separator, which reduces these interaction forces, allows higher acceleration rates to be achieved. However, such a ball separator must be designed to cope with significant dynamic forces.

It is apparent that the design and operation of standard rolling element bearings are not ideally suited to auxiliary applications, particularly in applications where oil based lubricants are inappropriate or ineffective. Accurate prediction of the durability of rolling element bearings under auxiliary operation still requires further analytical and experimental work. However, this study has identified that rolling element arrangements and component contact tribology are crucial factors.

Finally, it should be remarked that the identified problems of rolling element auxiliary bearing operation are avoided with alternative designs. In particular, planetary roller designs reduce the number of sliding contact within the bearing and therefore offer the potential for lower frictional losses and faster spin-up times.

ACKNOWLEDGEMENT

The authors gratefully acknowledge the support of the Engineering and Physical Sciences Research Council through Grant GR/L62238.

REFERENCES

1. Fumagalli, M. and Schweitzer, G., Measurements on a Rotor Contacting its Housing, 6th International Conference on *Vibrations in Rotating Machinery*, IMechE, Oxford, 1996, pp.779-788.
2. Ishii, T. and Kirk, R.G., Transient Response Technique Applied to Active Magnetic Bearing Machinery During Rotor Drop, *ASME Journal of Vibration and Acoustics*, 1996, Vol. 118, pp. 154-163.
3. Wang, X. and Noah, S., Nonlinear Dynamics of a Magnetically Supported Rotor on Safety Auxiliary Bearings, *ASME Journal of Vibration and Acoustics*, 1998, Vol. 120, pp. 596-606.
4. Kirk, R.G., Evaluation of AMB Turbomachinery Auxiliary Bearings, *ASME Journal of Vibration and Acoustics*, 1999, Vol. 121, pp. 156-161.
5. Lawen, J.L. and Flowers, G.T., Interaction Dynamics Between a Flexible Rotor and an Auxiliary Clearance Bearing, *ASME Journal of Vibration and Acoustics*, 1999, Vol. 121, pp.183-189.
6. Fumagalli, M., Varadi, P. and Schweitzer, G., Impact Dynamics of High Speed Rotors in Retainer Bearings and Measurement Concepts, 4th International Symposium on Magnetic Bearings, ETH, Zurich, 1994, pp. 239-244.
7. Gupta, P. K. Modelling of Instabilities Induced by Cage Clearances in Ball Bearings, *Tribology Transactions*, 1991, Vol. 34, pp. 93-99.
8. Stacke, L-E., Fritzson, D. and Nordling, P. BEAST - A Rolling Bearing Simulation Tool, *Proc. Instn. of Mech. Engrs, Part K, Journal of Multi-Body Dynamics*, 1999, Vol. 213, pp. 63-71.
9. Cole, M.O.T., Keogh, P.S. and Burrows, C.R., The Dynamic Behaviour of a Rolling Element Auxiliary Bearing, *ASME Journal of Tribology*, 2002, Vol. 124, pp. 406-413.
10. Dowson, D. and Higginson, G.R., *Elasto-hydrodynamic Lubrication*, Pergamon Press, 1966.